



Optimising nitrogen recovery from reject water in a 3-chamber bioelectroconcentration cell

Veera Koskue^{a,*}, Johanna M. Rinta-Kanto^a, Stefano Freguia^b, Pablo Ledezma^c, Marika Kokko^a

^a Faculty of Engineering and Natural Sciences, Tampere University, Korkeakoulunkatu 8, 33720 Tampere, Finland

^b Department of Chemical Engineering, The University of Melbourne, Grattan Street, Parkville, VIC 3010, Australia

^c Advanced Water Management Centre, The University of Queensland, Gehrman Laboratories Building (60), Brisbane, QLD 4072, Australia

ARTICLE INFO

Keywords:

Nutrient recovery
Reject water
Centrate
Bioelectroconcentration
Bioelectrochemical system

ABSTRACT

With the growing demand for macronutrients, such as nitrogen, and environmental issues related to their production, there is increasing need for efficient nutrient recycling. Reject waters from the dewatering of anaerobically digested sewage sludge are potential sources for nutrient recovery due to their high ammonium nitrogen ($\text{NH}_4\text{-N}$) concentration (ca. $1 \text{ g}_{\text{NH}_4\text{-N}} \text{ L}^{-1}$) and low volume (ca. 1% of incoming sewage). In this study, a 3-chamber bioelectroconcentration cell was used for $\text{NH}_4\text{-N}$ recovery into a liquid concentrate from both synthetic and real reject water. $\text{NH}_4\text{-N}$ recovery efficiency and rate were optimised based on $\text{NH}_4\text{-N}$ loading rate, varying from 1.4 to $9.4 \text{ g}_{\text{NH}_4\text{-N}} \text{ L}^{-1} \text{ d}^{-1}$ with synthetic reject water. The obtained $\text{NH}_4\text{-N}$ recovery efficiencies are the highest reported to date for bioelectroconcentration, peaking at $75.5 \pm 4.6\%$ (recovery rate of $728 \pm 117 \text{ g}_\text{N} \text{ m}^{-3} \text{ d}^{-1}$) at loading rate $1.9 \text{ g}_{\text{NH}_4\text{-N}} \text{ L}^{-1} \text{ d}^{-1}$. A loading rate of $2.9 \text{ g}_{\text{NH}_4\text{-N}} \text{ L}^{-1} \text{ d}^{-1}$ led to the most optimal ratio between $\text{NH}_4\text{-N}$ recovery efficiency ($68.2 \pm 11.6\%$) and recovery rate ($965 \pm 66 \text{ g}_\text{N} \text{ m}^{-3} \text{ d}^{-1}$), with $\text{NH}_4\text{-N}$ up-concentrated 7.4 ± 0.9 times to $7483 \pm 625 \text{ mg L}^{-1}$ in the concentrate. With real reject water, $\text{NH}_4\text{-N}$ recovery efficiency of $53.2 \pm 4.0\%$ and recovery rate of $556 \pm 37 \text{ g}_\text{N} \text{ m}^{-3} \text{ d}^{-1}$ were obtained at loading rate $2.5 \text{ g}_{\text{NH}_4\text{-N}} \text{ L}^{-1} \text{ d}^{-1}$, with a specific energy consumption of $6.1 \pm 1.1 \text{ kWh kg}_\text{N}^{-1}$. 16S rRNA amplicon analysis showed the dominance of phyla *Bacteroidetes* and *Firmicutes* in the anodic biofilms, with a significant change in the enriched microbial communities after transitioning from synthetic to real reject water. This study indicates the potential of bioelectroconcentration for nitrogen recovery from reject water without the need for an external organic carbon source or other chemical additions.

1. Introduction

Nutrients, especially the macronutrients nitrogen (N), phosphorus (P) and potassium (K), are extensively used as fertilisers in agriculture. However, chemical fertiliser production faces issues including finite resources, high energy demand and environmental damage [1]. For example, nitrogen conversion from atmospheric N_2 gas into plant-available ammonium nitrogen ($\text{NH}_4\text{-N}$) via the Haber-Bosch process requires $12.5 \text{ kWh kg}_\text{N}^{-1}$ [2], contributing up to 2% of the total global energy consumption annually [1]. In order to reduce the energy needs and emissions related to ammonium fertiliser production, more efficient nitrogen recycling is required. A potential source for recovering nitrogen

for reuse are municipal wastewaters that contain 11–30% of the nitrogen originally used as fertilisers [1,3,4].

In conventional wastewater treatment plants (WWTPs), nitrogen is largely removed by releasing it into the atmosphere as N_2 gas via biological nitrification/denitrification in the intensely aerated activated sludge process but it also partly accumulates in the activated sludge [2,5]. Excess activated sludge is collected for post-treatment, for which anaerobic digestion (AD) is one of the most widely applied processes. Nitrogen is largely re-solubilised during AD and when the digested sludge is dewatered, a nitrogen-rich (ca. $1000 \text{ mg NH}_4\text{-N L}^{-1}$) liquid fraction, i.e., reject water, is formed [5]. Reject water is commonly recirculated back to the head of the wastewater treatment process,

Abbreviations: AD, Anaerobic digestion; AEM, Anion-exchange membrane; BEC, Bioelectroconcentration cell; BES, Bioelectrochemical system; CEM, Cation-exchange membrane; COD, Chemical oxygen demand; EAM, Electroactive microorganisms; EC, Electrical conductivity; ED, Electrodialysis; L_N , Load ratio; OLR, Organic loading rate; sCOD, Soluble chemical oxygen demand; WWTP, Wastewater treatment plant.

* Corresponding author.

E-mail address: veera.koskue@tuni.fi (V. Koskue).

<https://doi.org/10.1016/j.seppur.2021.118428>

Received 2 December 2020; Received in revised form 27 January 2021; Accepted 30 January 2021

Available online 6 February 2021

1383-5866/© 2021 The Authors.

Published by Elsevier B.V. This is an open access article under the CC BY-NC-ND license

(<http://creativecommons.org/licenses/by-nc-nd/4.0/>).

which amounts up to 25% of the total $\text{NH}_4\text{-N}$ load to the WWTP [6,7]. As the energy demand for nitrogen removal from wastewater is ca. $12.5 \text{ kWh kg}_\text{N}^{-1}$ [2], reject water recirculation contributes significantly to the energy consumption and thus costs of the treatment. Developing novel technologies for nitrogen recovery from reject water, however, has the potential to simultaneously reduce or eliminate its additional $\text{NH}_4\text{-N}$ load to the overall WWTP process.

In recent years, nutrient recovery from liquid sources using bio-electrochemical systems (BES) has gained interest. In BESs, bacteria act as biocatalysts facilitating electrochemical reactions, such as converting chemical energy in organic matter into electrical energy [8]. Several bacterial groups, especially from phyla *Firmicutes* and *Proteobacteria*, have already been identified as electrochemically active, as recently reviewed [9]. The electrical energy generated with the help of bacteria can be directly used for nutrient recovery, making BESs a low-energy and chemical-free nutrient recovery device. By implementing a potential gradient between two electrodes, nutrients in ionic form can be forced to migrate through ion-selective membranes and form a concentrate. $\text{NH}_4\text{-N}$ can be concentrated from the anolyte into the catholyte through a cation-exchange membrane (CEM) in a 2-chamber set-up, after which the high pH (>10) resulting from the proton-consuming reduction reactions [10] can be exploited in the recovery of $\text{NH}_4\text{-N}$ via stripping, as soluble ammonium will increasingly transform into volatile ammonia (NH_3) gas [5,11]. Alternatively, a nutrient-rich liquid concentrate can be formed when pairing ion-exchange membranes [12,13].

Recent research regarding nitrogen recovery in BESs has focused on using human urine as a nutrient source. Urine has been considered an ideal electrolyte for BESs due to its high nutrient concentrations and low volume [11,14] as well as high ionic conductivity, buffer capacity and chemical oxygen demand (COD) content [15]. For example, a 3-chamber bioelectroconcentration cell (BEC) equipped with an ion-exchange membrane pair was able to effectively recover 50% of the influent $\text{NH}_4\text{-N}$ at a rate of $7.2 \text{ kg}_\text{N} \text{ m}^{-3} \text{ d}^{-1}$ from synthetic urine with an initial $\text{NH}_4\text{-N}$ concentration of 5.88 g L^{-1} [12]. The collection of human urine requires, however, the implementation of source-separating toilets and decentralised treatment facilities that are challenging to integrate into current wastewater infrastructure, especially in densely populated developed countries that have existing sewage collection systems [16]. Therefore, it is useful to assess how nutrient recovery from these centrally collected municipal wastewaters could be realised.

Reject waters from the anaerobic digesters of centralised WWTPs are concentrated streams with high $\text{NH}_4\text{-N}$ concentrations but volumes of only ca. 1% of the influent wastewater volume [6]. Reject waters have relatively high electrical conductivities (ECs) in the range of $6\text{--}17 \text{ mS cm}^{-1}$ [17,18], making them more favourable for use as electrolytes in BESs compared to the very dilute influent wastewaters entering the WWTPs. The low ionic conductivity of municipal wastewater ($1.3 \pm 0.1 \text{ mS cm}^{-1}$) was recently shown to limit both the obtainable current density ($<2 \text{ A m}^{-2}$) and $\text{NH}_4\text{-N}$ recovery (12.0%) from an initial $\text{NH}_4\text{-N}$ concentration of 63 mg L^{-1} in a 3-chamber BEC [13]. Reject waters have, however, been reported to be low in readily biodegradable organics [5], which poses a challenge for their treatment in BESs and has led to nitrogen recovery research being mainly carried out in abiotic electrochemical systems [18–21]. Alternatively, the COD content has been increased by feeding in organic-rich solutions separately or together with reject water to the anodes of BESs [5,22]. Furthermore, nutrient recovery from reject water in BESs has mainly been conducted in fed-batch mode [5,22]. From a practical point of view, it is beneficial to assess the applicability of reject water as the sole substrate in continuously-operated BESs.

The objective of this study was to concentrate nitrogen and other key nutrients, such as potassium, from reject water into a concentrated liquid fertiliser, while simultaneously reducing the nitrogen load to the WWTP caused by the recirculation of reject water. Nitrogen recovery was demonstrated from both synthetic and real reject water in a 3-

chamber BEC operated in continuous mode using reject water as the sole electrolyte. Initially, the nitrogen recovery efficiencies and rates using synthetic reject water were optimised based on $\text{NH}_4\text{-N}$ loading rate. Subsequently, real reject water from an anaerobic digester of a municipal WWTP was used as proof-of-concept for nitrogen recovery. The enriched microbial community of the bioanode was sampled and characterised to investigate its development under different experimental conditions and to identify potential electroactive and fermenting bacterial species.

2. Materials and methods

2.1. Experimental set-up

The experiments were carried out in duplicate 3-chamber BECs (Fig. 1) combining microbial electrolysis cell and electro dialysis (ED) technology [12]. Each chamber (anode, middle, and cathode) had a volume of 35 mL (total reactor volume 105 mL). EC-100 graphite granules (30 g dry weight; Graphite Sales, USA) and two graphite rods (diameter 6 mm, length 15 mm; Sigma-Aldrich, USA) were used as the anode and 35 cm^2 of AISI 304 stainless steel mesh (Tilox, Finland) with titanium wire as the cathode. The graphite granules were pre-treated as previously described [23]. Ag/AgCl reference electrodes in 3M NaCl (BASI, USA) were inserted directly into the anode and cathode chambers through Swagelok fittings for controlling or measuring electrode potential. With the electrodes in place, the initial hydraulic volumes of the anode and cathode chambers were 25 mL and 35 mL, respectively. All experiments were carried out in room temperature ($22\text{--}23 \text{ }^\circ\text{C}$).

During enrichment in batch mode, the reactors were operated as 2-chamber cells by placing a CEM (CMI-7000, Membranes International, USA) between the anode and middle chamber, creating a 35 mL anode chamber and a 70 mL cathode chamber. When switching to continuous mode, an anion-exchange membrane (AEM; AMI-7100, Membranes International, USA) was added between the middle and cathode chambers to complete the 3-chamber set-up (Fig. 1).

The two reactors were operated in chronoamperometric mode by applying a constant anode potential of 0.0 V vs. standard hydrogen electrode, corresponding to -0.209 V vs. Ag/AgCl in 3 M NaCl, with a VMP3 potentiostat (BioLogic, France). The generated current was continuously recorded with the potentiostat. Cathode potential was measured against the reference electrode in the cathode chamber and recorded with an Agilent 34970A datalogger (USA).

2.2. Media composition and bioanode enrichment

Both synthetic and real reject water were used as feed for the BEC. The enrichment of bioanodes was started with a synthetic reject water (SRW1) adapted from Modin et al. [24]. The recipe was modified by adding $500 \text{ mg L}^{-1} \text{ CH}_3\text{COONa}$, $1 \text{ g L}^{-1} \text{ 2-bromoethanesulfonic acid sodium salt (Na-BESA)}$; to inhibit possible methanogens present in the inoculum) and 1 mL L^{-1} trace element solution (see Supplementary Information).

Later, to imitate locally sourced reject water more closely, real reject water originating from a laboratory-scale anaerobic digester fed with municipal sewage sludge was characterised and an updated synthetic reject water recipe (SRW2) was formulated based on it, containing (in mg L^{-1}) $\text{CaCl}_2 \cdot 2\text{H}_2\text{O}$ (50), CH_3COOK (330), $\text{C}_2\text{H}_5\text{COONa}$ (658), KH_2PO_4 (3.1), KHCO_3 (292), $\text{MgSO}_4 \cdot 7\text{H}_2\text{O}$ (111), NH_4HCO_3 (6603) and 1 mL L^{-1} trace element solution. Na-BESA was no longer added to the feed. This updated synthetic reject water was used in the $\text{NH}_4\text{-N}$ loading rate optimisation experiments.

Finally, the BECs were fed with real reject water from Rahola municipal WWTP (Tampere, Finland), containing on average (mg L^{-1}) $\text{NH}_4\text{-N}$ (672), soluble COD (818), K^+ (101), Na^+ (56), Mg^{2+} (26), Ca^{2+} (59), Cl^- (56) and dissolved inorganic carbon (631). The reject water was pre-treated by centrifuging at 4500 rpm for 30 min and filtering the

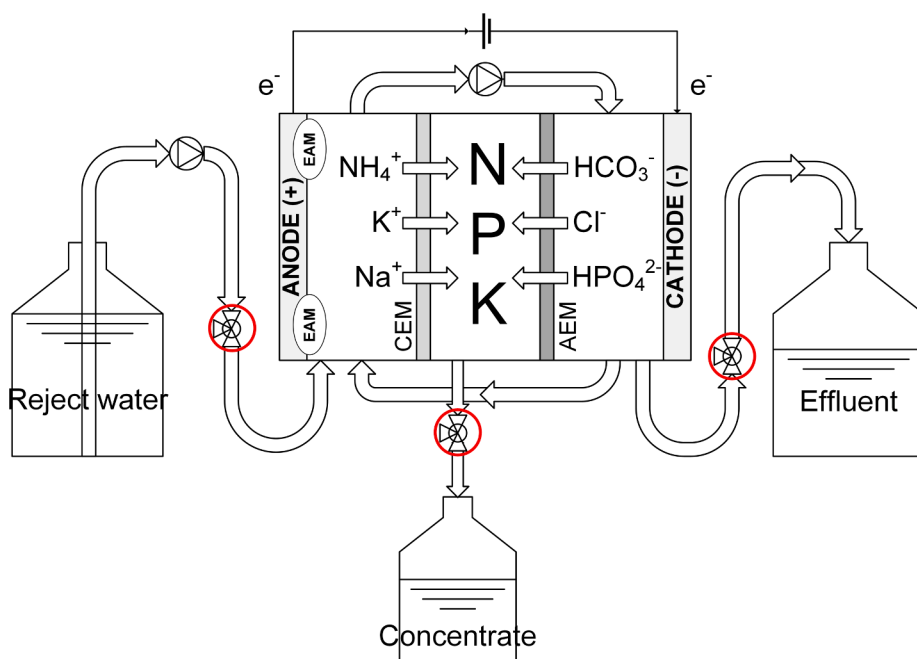


Fig. 1. Experimental set-up and operational principle of the continuously operated 3-chamber bioelectroconcentration cell. Reject water is pumped to the bioanode (EAM = electroactive microorganisms) and circulated to the cathode. Another pump is used to recirculate reject water back to the anode from the cathode. Concentrate is collected as overflow from the middle chamber, separated from the anode and cathode chambers by a cation-exchange membrane (CEM) and an anion-exchange membrane (AEM), respectively. Sampling points are marked in red. (For interpretation of the references to colour in this figure legend, the reader is referred to the web version of this article.)

supernatant through GF/A glass microfiber filters (Whatman, UK) to remove solid particles. Pre-treated reject water was stored at +4 °C prior to use.

For bioanode enrichment, the two reactors were inoculated with digested sewage sludge from Viinikanlahti municipal WWTP and composted biowaste from Tarastenjärvi municipal waste treatment facility (both in Tampere, Finland). The digested sewage sludge was roughly filtered through a loosely woven cloth and 1.5 mL of filtered sludge was mixed with a small amount of SRW1 and injected directly into the anode chamber. The composted biowaste was sieved through a 1 mm sieve and 1 g of the fine fraction was added to the bottom of the anode circulation bottle to prevent blocking the tubing with the solid particles. The operational conditions during bioanode enrichment are explained in detail in the [Supplementary Information](#).

2.3. Experimental operation and sampling

Experiments evaluating the effect of $\text{NH}_4\text{-N}$ loading rate on reactor performance were started with SRW2 after the reactors had been operated for 265 d. The $\text{NH}_4\text{-N}$ loading rate was step-wise increased from 1.4 to $9.4 \text{ g}_{\text{NH}_4\text{-N}} \text{ L}^{-1} \text{ d}^{-1}$ by increasing the feed rate ca. 1.5-fold for each

Table 1

Summary of the experimental operational parameters carried out with synthetic and real reject water. The $\text{NH}_4\text{-N}$ loading rates, organic loading rates (OLRs) and hydraulic retention times (HRTs) are normalised to the combined hydraulic volumes of the anode and cathode chambers (60 mL with synthetic and 49 mL with real reject water). The averaged $\text{NH}_4\text{-N}:\text{sCOD}$ ratios were 1.4 for synthetic and 0.8 for real reject water.

Experiment	Origin of reject water	Feed rate [mL h^{-1}]	$\text{NH}_4\text{-N}$ loading rate [$\text{g}_{\text{NH}_4\text{-N}} \text{ L}^{-1} \text{ d}^{-1}$]	OLR [$\text{g}_{\text{sCOD}} \text{ L}^{-1} \text{ d}^{-1}$]	HRT [h]
S1	Synthetic	3.2	1.4	1.0	20
S2	Synthetic	4.3	1.9	1.5	15
S3	Synthetic	6.1	2.9	2.1	9.8
S4	Synthetic	10.1	4.7	3.6	6.0
S5	Synthetic	14.6	6.8	5.9	4.1
S6	Synthetic	20.0	9.4	9.1	3.0
R1	Real	7.4	2.5	3.0	6.6
R2	Real	15.0	5.1	6.0	3.3

step (experiments S1–S6 in [Table 1](#)). Overall, six different loading rates were tested (normalised to the total hydraulic volume of the anode and cathode chambers, i.e., 60 mL), corresponding to six different HRTs and organic loading rates (OLRs), expressed as soluble COD (sCOD) content ([Table 1](#)). Additionally, two experiments were carried out with real reject water. The lower $\text{NH}_4\text{-N}$ loading rate of $2.5 \text{ g}_{\text{NH}_4\text{-N}} \text{ L}^{-1} \text{ d}^{-1}$ with real reject water (R1 in [Table 1](#)) was matched as closely as experimentally possible to the best-performing synthetic reject water runs and a second run was carried out with a higher $\text{NH}_4\text{-N}$ loading rate of $5.1 \text{ g}_{\text{NH}_4\text{-N}} \text{ L}^{-1} \text{ d}^{-1}$ (R2 in [Table 1](#)). Before starting the experiments with real reject water, glass pearls (6 mm diameter, acid-washed in 1 M HCl overnight) were added to the middle chambers of the BECs to support the membrane placement and avoid their deformation due to hydrostatic and osmotic pressures, which was observed in the experiments with synthetic reject water. In the experiments with real reject water, the hydraulic volume of the anode and cathode chambers had reduced slightly to 49 mL due to, e.g., biomass growth and precipitate formation in the anode chamber.

Throughout the experiments, anodic effluent was circulated to the cathode chamber and another pump was used to recirculate cathodic effluent back to the anode at 35 mL min^{-1} to maintain the buffer capacity and thus a close-to-neutral pH at the bioanode. The overflow from the cathode was collected into an effluent bottle and the overflow from the middle chamber (formed due to osmotic and electro-osmotic water flows) into a concentrate bottle ([Fig. 1](#)).

After each change in operational parameters, reactor performance was allowed to stabilize for at least four HRTs until current generation seemed to visually plateau and the change in the EC of consecutive concentrate samples was $\leq 5\%$ compared to the average of the samples, indicating steady-state conditions. At steady-state, samples were taken from feed, effluent and middle chamber (see sampling points marked in red in [Fig. 1](#)) three times with 8–48 h time intervals between samplings. Effluent and concentrate volumes were determined by weight.

2.4. Chemical analyses

EC and pH of all samples were measured immediately after sampling using LAQUAtwin probes B-771 and B-712 (Horiba Scientific, Japan), respectively. Samples were filtered through Chromafil Xtra PET syringe filters (pore size $0.20 \mu\text{m}$ for synthetic and $0.45 \mu\text{m}$ for real reject water

samples; Macherey-Nagel, Germany) and $\text{NH}_4\text{-N}$ was immediately measured with LCK304 cuvette test kits using a DR 2800 spectrophotometer (HACH, USA). For other analyses, filtered samples were stored at -20°C .

K^+ , Na^+ , Mg^{2+} and Ca^{2+} were determined according to standard SFS-EN ISO 14911 using Dionex DX-120 ion chromatograph with AS40 autosampler, IonPac CS12A cation exchange column, CSRS 300 suppressor (4 mm) (Thermo Fisher Scientific, USA) and 20 mM methanesulfonic acid as eluent at 1 mL min^{-1} . $\text{PO}_4\text{-P}$, $\text{SO}_4\text{-S}$ and Cl^- were determined according to standard SFS-EN ISO 10304-1 using Dionex ICS-1600 ion chromatograph with AS-DV autosampler and ASRS 300 suppressor (4 mm) (Thermo Fisher Scientific, USA). Either IonPac AS4A-SC anion exchange column with $1.9\text{ mM Na}_2\text{CO}_3/1.7\text{ mM NaHCO}_3$ as eluent at 1 mL min^{-1} or IonPac AS22 anion exchange column with $4.5\text{ mM Na}_2\text{CO}_3/1.4\text{ mM NaHCO}_3$ as eluent at 1.2 mL min^{-1} was used. Dissolved inorganic carbon (DIC) was determined according to standard SFS-EN 1484 using TOC-5000 total organic carbon analyser with ASI-5000 autosampler (Shimadzu, Japan). Volatile fatty acids (VFAs) were measured with GC-2010 Plus Capillary gas chromatograph with AOC-20i auto injector (Shimadzu, Japan), equipped with a Zebron ZB-WAX column (Phenomenex, USA) and a flame ionization detector (FID) as described before [25]. For real reject water, soluble chemical oxygen demand (sCOD) was determined using the dichromate method according to standard SFS 5504. For calculations and statistical analysis of the results, see [Supplementary Information](#).

2.5. Microbial community analyses

Samples for microbial community analyses were collected from the two inocula and from both anode chambers (approx. time of operation in months) after continuous operation with synthetic reject water (11) and after continuous operation with real reject water (16). Anodic biofilm samples were taken by loosely filling 15 mL Falcon centrifuge tubes with biofilm-covered granules from the anode compartments of the BECs and storing them at -80°C . After thawing the samples, biofilm was detached from the granules by ultrasonication in 0.05 M phosphate buffer (pH 7.1) for $5 \times 1\text{ min}$ (with 30 s breaks in between) using a Soniprep 150 Plus tip sonicator (MSE Centrifuges, UK) at approx. 40% of maximum amplitude. 10 mL of the phosphate buffer containing the suspended biomass was centrifuged at 7 500 G for 10 min and the separated solid biomass was re-suspended into 1.5 mL of the same buffer before submission for DNA extraction. Inoculum samples were also stored at -80°C and submitted for DNA extraction as such. Details about DNA extraction and microbial data processing can be found in the [Supplementary Information](#). The raw sequence data were uploaded to open source metagenomics web application server MG-RAST [26] and can be accessed in their data depository [27].

3. Results and discussion

3.1. $\text{NH}_4\text{-N}$ recovery efficiency and rate

With synthetic reject water, the highest $\text{NH}_4\text{-N}$ recovery efficiency of $75.5 \pm 4.6\%$ was obtained at $\text{NH}_4\text{-N}$ loading rate of $1.9\text{ g}_{\text{NH}_4\text{-N}}\text{ L}^{-1}\text{ d}^{-1}$ (Fig. 2A and [Supplementary Information Table S1](#)). Similarly, other low loading rates of 1.4 and $2.9\text{ g}_{\text{NH}_4\text{-N}}\text{ L}^{-1}\text{ d}^{-1}$ led to high $\text{NH}_4\text{-N}$ recovery efficiencies of $66.6 \pm 11.5\%$ and $68.2 \pm 11.6\%$, respectively. When the $\text{NH}_4\text{-N}$ loading rate was increased further, the $\text{NH}_4\text{-N}$ recovery efficiency clearly declined. With the highest loading rates of 6.8 and $9.4\text{ g}_{\text{NH}_4\text{-N}}\text{ L}^{-1}\text{ d}^{-1}$, the $\text{NH}_4\text{-N}$ recovery efficiencies were $25.6 \pm 4.0\%$ and $27.1 \pm 6.8\%$, respectively. Conversely, the $\text{NH}_4\text{-N}$ recovery rates increased with increasing $\text{NH}_4\text{-N}$ loading rate, ranging from $551 \pm 67\text{ g}_\text{N}\text{ m}^{-3}\text{ d}^{-1}$ (normalised to total reactor volume, 105 mL; or $17 \pm 2\text{ g}_\text{N}\text{ m}^{-2}\text{ d}^{-1}$, normalised to effective membrane surface area, 35 cm^2) to $1254 \pm 339\text{ g}_\text{N}\text{ m}^{-3}\text{ d}^{-1}$ ($38 \pm 10\text{ g}_\text{N}\text{ m}^{-2}\text{ d}^{-1}$) (Fig. 2B). The $\text{NH}_4\text{-N}$ loading rate of $2.9\text{ g}_{\text{NH}_4\text{-N}}\text{ L}^{-1}\text{ d}^{-1}$ was found to lead to the most optimal combination

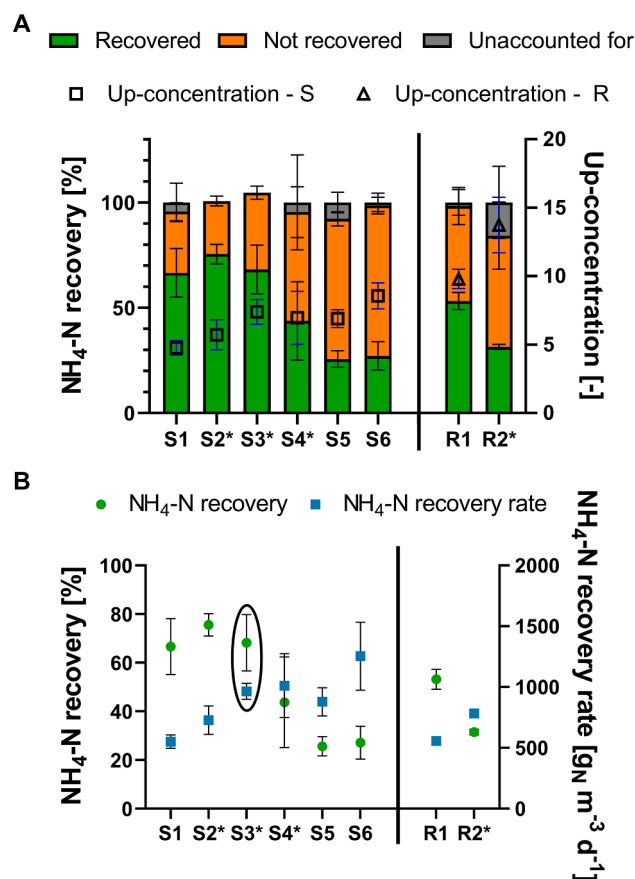


Fig. 2. A) $\text{NH}_4\text{-N}$ mass balances (bars) and up-concentration factors (scatter) in the experiments with differing $\text{NH}_4\text{-N}$ loading rates with synthetic (S1–S6) and real (R1–R2) reject water (for experimental parameters, see [Table 1](#)). B) $\text{NH}_4\text{-N}$ recovery efficiencies and recovery rates in the different experiments. The best recovery efficiency to recovery rate ratio with synthetic reject water was obtained in experiment S3 with the $\text{NH}_4\text{-N}$ loading rate of $2.9\text{ g}_{\text{NH}_4\text{-N}}\text{ L}^{-1}\text{ d}^{-1}$ (circled). *Results from only one of the duplicate reactors taken into account due to operational issues with the second reactor.

of total $\text{NH}_4\text{-N}$ recovery ($68.2 \pm 11.6\%$) and $\text{NH}_4\text{-N}$ recovery rate ($965 \pm 66\text{ g}_\text{N}\text{ m}^{-3}\text{ d}^{-1}$, or $29 \pm 2\text{ g}_\text{N}\text{ m}^{-2}\text{ d}^{-1}$).

With real reject water, the $\text{NH}_4\text{-N}$ recovery was $53.2 \pm 4.0\%$ at loading rate of $2.5\text{ g}_{\text{NH}_4\text{-N}}\text{ L}^{-1}\text{ d}^{-1}$, decreasing to $31.4 \pm 1.2\%$ at loading rate of $5.1\text{ g}_{\text{NH}_4\text{-N}}\text{ L}^{-1}\text{ d}^{-1}$ (Fig. 2A). Similar to the synthetic reject water experiments, a higher $\text{NH}_4\text{-N}$ recovery rate of $783 \pm 10\text{ g}_\text{N}\text{ m}^{-3}\text{ d}^{-1}$ (or $23 \pm 0.3\text{ g}_\text{N}\text{ m}^{-2}\text{ d}^{-1}$) was obtained with the higher loading rate, compared to $556 \pm 37\text{ g}_\text{N}\text{ m}^{-3}\text{ d}^{-1}$ ($17 \pm 1\text{ g}_\text{N}\text{ m}^{-2}\text{ d}^{-1}$) at the lower loading rate (Fig. 2B). The $\text{NH}_4\text{-N}$ recovery efficiencies and recovery rates were lower with real reject water than with synthetic reject water. When comparing to the synthetic runs with the closest matching $\text{NH}_4\text{-N}$ loading rates (runs S3 and S4, Fig. 2), the obtained $\text{NH}_4\text{-N}$ recovery efficiencies were 22–28% and $\text{NH}_4\text{-N}$ recovery rates 23–42% lower with real reject water, suggesting the optimised operational parameters for synthetic reject water do not directly apply to real reject water. The reduced performance with real reject water is likely because of the 11–31% lower current densities (see [Section 3.3](#) and [Table S1](#)) compared to the synthetic runs, generating less electrostatic force to drive the bioelectroconcentration of $\text{NH}_4\text{-N}$. The lower current densities observed in the experiments with real reject water were likely a result of the electric conductivity of real reject water ($5.7 \pm 0.2\text{ mS cm}^{-1}$; [Table 2](#)) being 27% lower than that of the synthetic reject water ($7.8 \pm 0.5\text{ mS cm}^{-1}$), as the difference is in the same range as the discrepancy in the $\text{NH}_4\text{-N}$ recovery efficiencies and rates. Additionally, the lower amount of readily bioavailable organics, such as acetate and propionate,

Table 2

Properties of the synthetic and real reject water feeds and the concentrates obtained in the optimised runs. The up-concentration factor tells how many times higher the concentrate value is compared to the feed.

Parameter [unit]	Synthetic reject water with $\text{NH}_4\text{-N}$ loading rate $2.9 \text{ g}_{\text{NH}_4\text{-N}} \text{ L}^{-1} \text{ d}^{-1}$ *			Real reject water with $\text{NH}_4\text{-N}$ loading rate $2.5 \text{ g}_{\text{NH}_4\text{-N}} \text{ L}^{-1} \text{ d}^{-1}$		
	Feed	Concentrate	Up-concentration	Feed	Concentrate	Up-concentration
pH [-]	8.0 ± 0.0	7.9 ± 0.0	–	7.8 ± 0.2	7.9 ± 0.0	–
EC [mS cm^{-1}]	7.8 ± 0.5	38.3 ± 0.8	4.9 ± 0.2	5.7 ± 0.2	35.3 ± 2.0	6.3 ± 0.5
$\text{NH}_4\text{-N}$ [mg L^{-1}]	1015 ± 48	7483 ± 625	7.4 ± 0.9	665 ± 7	6508 ± 438	9.8 ± 0.7
K [mg L^{-1}]	267 ± 3	1880 ± 5	7.0 ± 0.1	107 ± 11	1050 ± 95	10.0 ± 1.6
Na [mg L^{-1}]	164 ± 2	1119 ± 6	6.8 ± 0.0	59 ± 2	714 ± 86	12.3 ± 1.8
Mg [mg L^{-1}]	16 ± 0.5	150 ± 8	9.5 ± 0.3	28 ± 1	515 ± 28	18.7 ± 0.8
Ca [mg L^{-1}]	20 ± 1	17 ± 2	0.9 ± 0.1	61 ± 6	30 ± 6	0.5 ± 0.1
Cl [mg L^{-1}]	18 ± 2	162 ± 3	9.0 ± 1.0	56 ± 2	906 ± 80	16.2 ± 1.8
$\text{SO}_4\text{-S}$ [mg L^{-1}]	10 ± 0.05	n.d.	n.a.	0.53 ± 0.04	n.d.	n.a.
sCOD [mg L^{-1}]	n.a.	n.a.	n.a.	844 ± 48	2192 ± 110	2.6 ± 0.2
Acetate [mg L^{-1}]	152 ± 3.1	1154 ± 45	7.6 ± 0.2	80 ± 9.1	1018 ± 81	13.4 ± 2.5
Propionate [mg L^{-1}]	468 ± 3.2	2318 ± 22	5.0 ± 0.1	51 ± 3.7	205 ± 14	4.0 ± 0.5
DIC [mg L^{-1}]	4539 ± 4.4	31785 ± 414	7.0 ± 0.1	631 ± 15	5184 ± 487	8.4 ± 0.7

n.d. = not detected; n.a. = not applicable.

*results from only one of the duplicate reactors taken into account due to operational issues with the second reactor ($n = 3$).

in real reject water compared to the synthetic reject water (see Table 2) potentially contributed to the reduced electricity generation.

It was recently proposed that $\text{NH}_4\text{-N}$ load ratio (L_N), i.e., the ratio between the current and the $\text{NH}_4\text{-N}$ loading rate (Eq. S2) in a (B)ES, is an important parameter in determining the $\text{NH}_4\text{-N}$ recovery and energy input of a recovery system [28,29]. When $L_N < 1$, the applied/obtained current is not enough to transport all $\text{NH}_4\text{-N}$ and at $L_N > 1$, there is excess current in relation to the $\text{NH}_4\text{-N}$ loading rate. The application of the load ratio is simpler with electrochemical systems where the current can be more easily controlled but it has been found to be applicable for BESs as well [29].

Here, the current was generated by the anodic biofilm and not controlled, and therefore the load ratios could only be determined afterwards based on the measured current (Eq. S2). As mentioned above, the current densities obtained with real reject water were lower than with synthetic reject water, which also resulted in the load ratios remaining < 1 for real reject water, whereas they were in the range 1.3–1.4 in the best-performing runs with synthetic reject water (Table S1). The generated current was thus not enough to transport all $\text{NH}_4\text{-N}$ across the CEM in the experiments with real reject water. Increasing the load ratio above 1 also for real reject water would be vital for obtaining higher $\text{NH}_4\text{-N}$ recovery efficiency, and this could be done either by increasing the generated current and/or reducing the $\text{NH}_4\text{-N}$ loading rate. From both the results with synthetic and real reject water, it could be seen that lower $\text{NH}_4\text{-N}$ loading rates led to higher load ratios (Table S2). Reducing the $\text{NH}_4\text{-N}$ loading rate further with real reject water could therefore lead to a desired load ratio > 1 . The $\text{NH}_4\text{-N}$ loading rates (and thus feed rates) studied here were, however, already very low and it would not be desirable to reduce them much further, as this would cause the HRT to increase, increasing the reactor volume in larger-scale applications. A more feasible approach could therefore be to increase the current generation e.g. by mixing the reject water with an external COD source, as has been done before [22].

Despite not being able to remove and recover all influent $\text{NH}_4\text{-N}$, the hereby obtained recovery efficiencies would already mean significant reductions to the WWTP $\text{NH}_4\text{-N}$ load caused by reject water recirculation back to the beginning of the treatment. The results also show that by optimising $\text{NH}_4\text{-N}$ loading rates, it was possible to obtain higher $\text{NH}_4\text{-N}$ recovery efficiencies with both synthetic and real reject water than previously reported for a similar BEC run with synthetic urine (49.5 \pm 1.8%) [12] and real municipal wastewater (12.0 \pm 1.4%) [13]. Recently, Barua et al. [22] obtained high total $\text{NH}_4\text{-N}$ recovery when $\text{NH}_4\text{-N}$ was concentrated from anode to cathode on average at 53 \pm 5% efficiency in a 2-chamber BES, followed by an additional 38 \pm 3% recovery into struvite after magnesium addition to the anode effluent. In order to obtain this result, however, the real reject water used had to be

mixed with COD-rich primary sludge fermentation liquor [22]. Wu and Modin [5] also used a 2-chamber BES to increase the pH of reject water at the cathode before recovering up to 94% of $\text{NH}_4\text{-N}$ from synthetic and 79% from real reject water in a separate stripping and absorption unit. A purely electrochemical decoupled ED system obtained 92% $\text{NH}_4\text{-N}$ removal from synthetic and 75% removal from real reject water but only a small fraction was effectively recovered as the *in situ* generated H_2 was not enough to strip ammonia from the basic catholyte [21]. In a pilot-scale electrochemical 30-pair ED stack system fed with municipal reject water after pre-treatment in a struvite crystalliser system, $\text{NH}_4\text{-N}$ recovery into a liquid concentrate remained relatively low at 23 \pm 3% [20]. The recovery efficiencies obtained here indicate that the performance of the studied BEC is comparable to many other (bio)electrochemical systems used for nutrient recovery from reject water, and the results were obtained with no external COD addition or use of other chemicals.

3.2. Up-concentration and concentrate characteristics

The highest $\text{NH}_4\text{-N}$ up-concentration factors, i.e., the concentrate concentration divided by influent concentration, were obtained at the highest applied $\text{NH}_4\text{-N}$ loading rates. $\text{NH}_4\text{-N}$ up-concentrations peaked at 8.6 ± 1.2 at $\text{NH}_4\text{-N}$ loading rate of $9.4 \text{ g}_{\text{NH}_4\text{-N}} \text{ L}^{-1} \text{ d}^{-1}$ for synthetic and at 13.7 ± 1.2 at loading rate of $5.1 \text{ g}_{\text{NH}_4\text{-N}} \text{ L}^{-1} \text{ d}^{-1}$ for real reject water (Fig. 2A). The higher up-concentration factors for real reject water were a consequence of the lower $\text{NH}_4\text{-N}$ concentrations in the feed ($672 \text{ g}_{\text{NH}_4\text{-N}} \text{ L}^{-1}$ in real reject water compared to $1170 \text{ g}_{\text{NH}_4\text{-N}} \text{ L}^{-1}$ in the synthetic reject water).

In order to study the quality of the produced liquid concentrate in detail and its potential for fertiliser use, the synthetic and real reject water feeds and concentrates were fully characterised for the experiments with the optimal $\text{NH}_4\text{-N}$ loading rates (2.9 and $2.5 \text{ g}_{\text{NH}_4\text{-N}} \text{ L}^{-1} \text{ d}^{-1}$ for synthetic and real reject water, respectively) and up-concentration factors were determined for different compounds (Table 2). As mentioned above, up-concentration factors were higher for real reject water due to lower influent concentrations. The conductivities of the concentrates reached 38.3 ± 0.5 and $35.3 \pm 2.4 \text{ mS cm}^{-1}$ with synthetic and real reject water, respectively. In these runs with optimal $\text{NH}_4\text{-N}$ loading rates, $\text{NH}_4\text{-N}$ was up-concentrated 7.4 ± 0.5 times to $7483 \pm 370 \text{ mg L}^{-1}$ with synthetic reject water and 9.8 ± 0.9 times to $6508 \pm 533 \text{ mg L}^{-1}$ with real reject water.

Another key nutrient, potassium (K^+), was up-concentrated to $1880 \pm 5 \text{ mg L}^{-1}$ with synthetic and to $1050 \pm 95 \text{ mg L}^{-1}$ with real reject water (Table 2), with recovery efficiencies of $64.9 \pm 8.0\%$ and $48.4 \pm 12.9\%$, respectively (Fig. S1). The third macronutrient of interest, $\text{PO}_4\text{-P}$, was not detected in the reject water. The WWTP from which the reject

water was obtained uses chemical phosphorus removal, leading to the insoluble phosphate salts largely staying in the solid fraction of the dewatered digested sewage sludge [30] and therefore to negligible concentrations in the reject water.

With regards to other minor nutrients, with both synthetic and real reject water, magnesium (Mg^{2+}) was concentrated most efficiently into the concentrate, with up-concentration factors of 9.5 ± 0.3 and 18.7 ± 0.8 , respectively (Table 2). Of all the studied ions, magnesium also had the highest recovery efficiencies for synthetic ($87.6 \pm 9.0\%$) and real ($88.1 \pm 6.2\%$) reject water (Fig. S1). Conversely, hardly any calcium (Ca^{2+}) was detected in the concentrate despite having the same + 2 charge, with only $8.1 \pm 1.2\%$ and $2.9 \pm 0.5\%$ recoveries for synthetic and real reject water, respectively, and concentrations lower than in the feed (up-concentration factors < 1). In fact, most of the calcium was lost in the system (Fig. S1) likely due to its precipitation as calcium carbonate, CaCO_3 . Indeed, a white precipitate was seen to form in the reactors with both synthetic and real reject waters. Precipitation can cause issues with, e.g., tube and pipe clogging, and therefore a pre-treatment to remove calcium prior to the nutrient recovery process could be considered. Furthermore, both magnesium and calcium can potentially contribute to membrane scaling, which in turn may increase the internal resistance and thus cell voltage. Here, the membranes were changed periodically and no long-term data about the evolution of the internal resistance and cell voltage is available, but scaling in membrane systems operated with reject water has been extensively studied elsewhere [31].

Special attention should also be paid to the concentrations of sodium (Na^+) and chloride (Cl^-) which can cause salination of soil and thus decrease agricultural production [32]. These ions were concentrated into the middle chamber with high up-concentration factors (Table 2) but their final concentrations in the concentrate (for sodium, 1119 ± 6 and $714 \pm 86 \text{ mg L}^{-1}$ with synthetic and real reject water, respectively, and for chloride, 162 ± 3 and $906 \pm 80 \text{ mg L}^{-1}$ with synthetic and real reject water, respectively) were significantly lower compared to $\text{NH}_4\text{-N}$ due to their lower initial concentrations. Previously, the direct application of reject water originating from anaerobically digested cow slurry has been found to produce similar or improved yields when compared to inorganic fertilisers, while simultaneously reducing the potential of nutrient losses to the environment [33], suggesting that liquid fertilisers derived from digestates could be used for agricultural purposes. Nevertheless, the suitability of the recycled nutrients to be used as fertilisers should be studied separately.

3.3. Current generation and organics removal

In the experiments with optimal $\text{NH}_4\text{-N}$ loading rates, the current densities were $3.7 \pm 0.6 \text{ A m}^{-2}$ (relative to effective membrane surface area) at $\text{NH}_4\text{-N}$ loading rate of $2.9 \text{ g}_{\text{NH}_4\text{-N}} \text{ L}^{-1} \text{ d}^{-1}$ with synthetic reject water and $2.5 \pm 0.2 \text{ A m}^{-2}$ at loading rate of $2.5 \text{ g}_{\text{NH}_4\text{-N}} \text{ L}^{-1} \text{ d}^{-1}$ with real reject water (Table S1). The highest current densities were obtained with the highest $\text{NH}_4\text{-N}$ loading rates studied, reaching $4.8 \pm 0.8 \text{ A m}^{-2}$ at $9.4 \text{ g}_{\text{NH}_4\text{-N}} \text{ L}^{-1} \text{ d}^{-1}$ for synthetic and $4.0 \pm 1.2 \text{ A m}^{-2}$ at $5.1 \text{ g}_{\text{NH}_4\text{-N}} \text{ L}^{-1} \text{ d}^{-1}$ for real reject water. When comparing to the theoretical maximum current densities calculated based on the applied OLRs, the current densities in the optimised runs were 65% of the theoretical maximum at $\text{NH}_4\text{-N}$ loading rate of $2.9 \text{ g}_{\text{NH}_4\text{-N}} \text{ L}^{-1} \text{ d}^{-1}$ (corresponding to an OLR of $2.1 \text{ g}_{\text{sCOD}} \text{ L}^{-1} \text{ d}^{-1}$; see Table 1) with synthetic and 42% at $2.5 \text{ g}_{\text{NH}_4\text{-N}} \text{ L}^{-1} \text{ d}^{-1}$ (or $3.0 \text{ g}_{\text{sCOD}} \text{ L}^{-1} \text{ d}^{-1}$) with real reject water. At the highest $\text{NH}_4\text{-N}$ loading rates this decreased further, the current densities being only 26% of the theoretical maximum at $9.4 \text{ g}_{\text{NH}_4\text{-N}} \text{ L}^{-1} \text{ d}^{-1}$ (or $9.1 \text{ g}_{\text{sCOD}} \text{ L}^{-1} \text{ d}^{-1}$) with synthetic and 36% at $5.1 \text{ g}_{\text{NH}_4\text{-N}} \text{ L}^{-1} \text{ d}^{-1}$ (or $6.0 \text{ g}_{\text{sCOD}} \text{ L}^{-1} \text{ d}^{-1}$) with real reject water. The current densities with real reject water were, however, considerably higher than recently reported by Barua et al. [22], whose 2-chamber BES was only able to generate current densities < 0.15 A m^{-2} with real reject water as the only substrate, leading also to negligible nitrogen recovery.

At the same time, sCOD removal was only in the range of 6–24% with

both synthetic and real reject water, with the exception of experiment with real reject water at $\text{NH}_4\text{-N}$ loading rate of $5.1 \text{ g}_{\text{NH}_4\text{-N}} \text{ L}^{-1} \text{ d}^{-1}$ where the results indicated an increase in the sCOD concentration from the influent to the effluent, for which no explanation could be found. The organics removals were in the same range with recent findings by Barua et al. (2019), who observed sCOD removals of 14–26% in fed-batch cycles with a significantly higher HRT of 123 h with real reject water as the sole substrate. In the current study, the Coulombic efficiencies based on sCOD removal were extremely high (>100% for all runs), suggesting sCOD was not the only compound being oxidized at the anode and thus contributing to current generation. A known explanation for this is the oxidation of H_2 produced at the cathode and transported to the anode due to the continuous recirculation between the two chambers [34].

3.4. Charge transport and energy requirement

$\text{NH}_4\text{-N}$ (50–71%) and HCO_3^- (49–74%) were the ions responsible for the majority of charge transport over the CEM and AEM, respectively, with both synthetic and real reject water at different $\text{NH}_4\text{-N}$ loading rates (Fig. 3). Increasing $\text{NH}_4\text{-N}$ loading rate was seen to increase $\text{NH}_4\text{-N}$ transport efficiency as well as obtained current density (Table S1). A two-factor analysis of variance (ANOVA) showed that the origin of the feed (synthetic or real reject water; $p = 0.0097$) and $\text{NH}_4\text{-N}$ loading rate ($p = 0.0023$) had a statistically relevant effect on the transport efficiency. As the increasing $\text{NH}_4\text{-N}$ loading rate led to a decrease in load ratio, i.e., ratio between obtained current density and $\text{NH}_4\text{-N}$ loading rate (Table S1), the contribution of $\text{NH}_4\text{-N}$ to the charge transport followed a decreasing trend with increasing load ratio, which is in line with previous observations [35,36]. Overall, the obtained current was more efficiently used for $\text{NH}_4\text{-N}$ concentration than previously seen with real reject water in two different types of electrochemical systems fed with real reject water, in which $\text{NH}_4\text{-N}$ contributed to 40% of the total charge transport both in a laboratory-scale 2-chamber stripping set-up [18] and a pilot-scale ED system [20].

Even though other ions were found to concentrate into the middle chamber at least as efficiently as $\text{NH}_4\text{-N}$ and HCO_3^- , they only contributed to low percentages of the total charge transport due to their initial concentrations being order(s) of magnitude lower than those of $\text{NH}_4\text{-N}$ and HCO_3^- (Fig. 3). Furthermore, a significant portion of the charge transport over both membranes could not be explained by the analysed

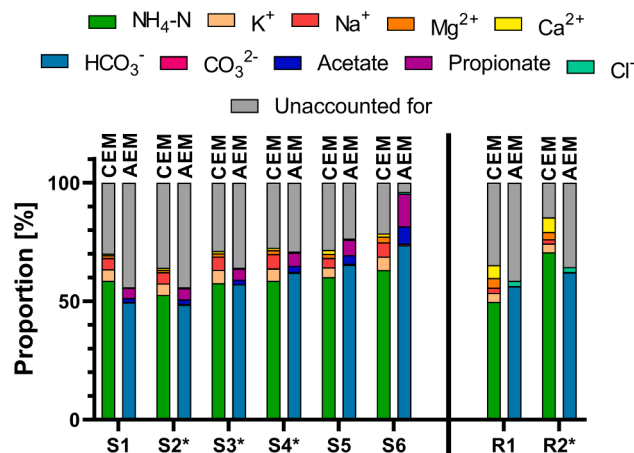


Fig. 3. Contribution of the different ions to the charge transport over the cation exchange membrane (CEM) and anion exchange membrane (AEM) in the different experiments with synthetic (S1–S6) or real (R1–R2) reject water (for experimental parameters, see Table 1). Increasing $\text{NH}_4\text{-N}$ loading rate was found to increase the $\text{NH}_4\text{-N}$ transport efficiency. *Results from only one of the duplicate reactors taken into account due to operational issues with the second reactor.

ions. Some of this could be explained by the migration of H^+ or OH^- into the middle chamber, which is what e.g. Kuntke et al. [34,35] assumed happened in their 2-chamber system over the CEM. However, another likely explanation is the leakage of counter-ions through the membranes, i.e., ions that have been concentrated into the middle chamber through one membrane escape the middle chamber through the other membrane. Indeed, previous findings suggest this plays a significant role in the charge transport, with leakage of the concentrated NH_4-N from the middle chamber into the cathode through the AEM reported ranging from 10% with synthetic urine [12] up to 39% with real municipal wastewater [13]. This phenomenon is mainly due to the insufficient perm-selectivity of the membranes as well as large concentration gradients between the chambers, leading to back-diffusion of ion pairs [12,20].

The NH_4-N transport efficiency is an important parameter affecting the energy requirement for NH_4-N recovery [34]. Here, the electrical energy needed for nitrogen recovery was determined for the experiments carried out with real reject water. The energy requirement was $6.1 \pm 1.1 \text{ kWh kg}_N^{-1}$ at NH_4-N loading rate of $2.5 \text{ g}_{NH_4-N} \text{ L}^{-1} \text{ d}^{-1}$ and $8.2 \pm 3.1 \text{ kWh kg}_N^{-1}$ at $5.1 \text{ g}_{NH_4-N} \text{ L}^{-1} \text{ d}^{-1}$, excluding electricity used for pumping and pre-treatment of the reject water. As explained by Ward et al. [20], the additional energy consumption due to the pumping can be fairly high in small-scale set-ups due to the use of peristaltic pumps,

but the pumping energy requirement can be expected to be an order of magnitude lower than the electrochemical energy input in larger scale, and is therefore not considered here. With the higher loading rate $5.1 \text{ g}_{NH_4-N} \text{ L}^{-1} \text{ d}^{-1}$, there was more variation of the generated current and cell voltage (see Fig. S2) which was likely caused by the EC of the effluent linearly decreasing from 4.5 to 2.8 mS cm^{-1} over the course of the experiment. With the loading rate $2.5 \text{ g}_{NH_4-N} \text{ L}^{-1} \text{ d}^{-1}$, the effluent EC, and thus the current generation and cell voltage, remained relatively stable.

The $6.1 \pm 1.1 \text{ kWh kg}_N^{-1}$ obtained at NH_4-N loading rate of $2.5 \text{ g}_{NH_4-N} \text{ L}^{-1} \text{ d}^{-1}$ is very close to the $5.8 \pm 0.1 \text{ kWh kg}_N^{-1}$ obtained by Barua et al. [22] in a 2-chamber BES, with an almost identical NH_4-N removal/recovery efficiency ($53 \pm 5\%$ vs. $53.2 \pm 4.0\%$ obtained here) for a mixture of reject water and primary sludge fermentation liquor. In a pilot-scale abiotic ED cell with 30 cell pairs treating real reject water, Ward et al. [20] were able to get the electrical energy consumption down to $4.9 \pm 1.5 \text{ kWh kg}_N^{-1}$. However, the overall NH_4-N recovery efficiency remained low at $23 \pm 3\%$ and the system required chemical additions [20]. In the current study, the obtained transport efficiencies of NH_4-N were relatively high, suggesting the produced current is already efficiently used for NH_4-N concentration. In order to bring the energy requirement further down, the focus should be on minimising electrochemical losses and particularly the cell voltage via, e.g., the

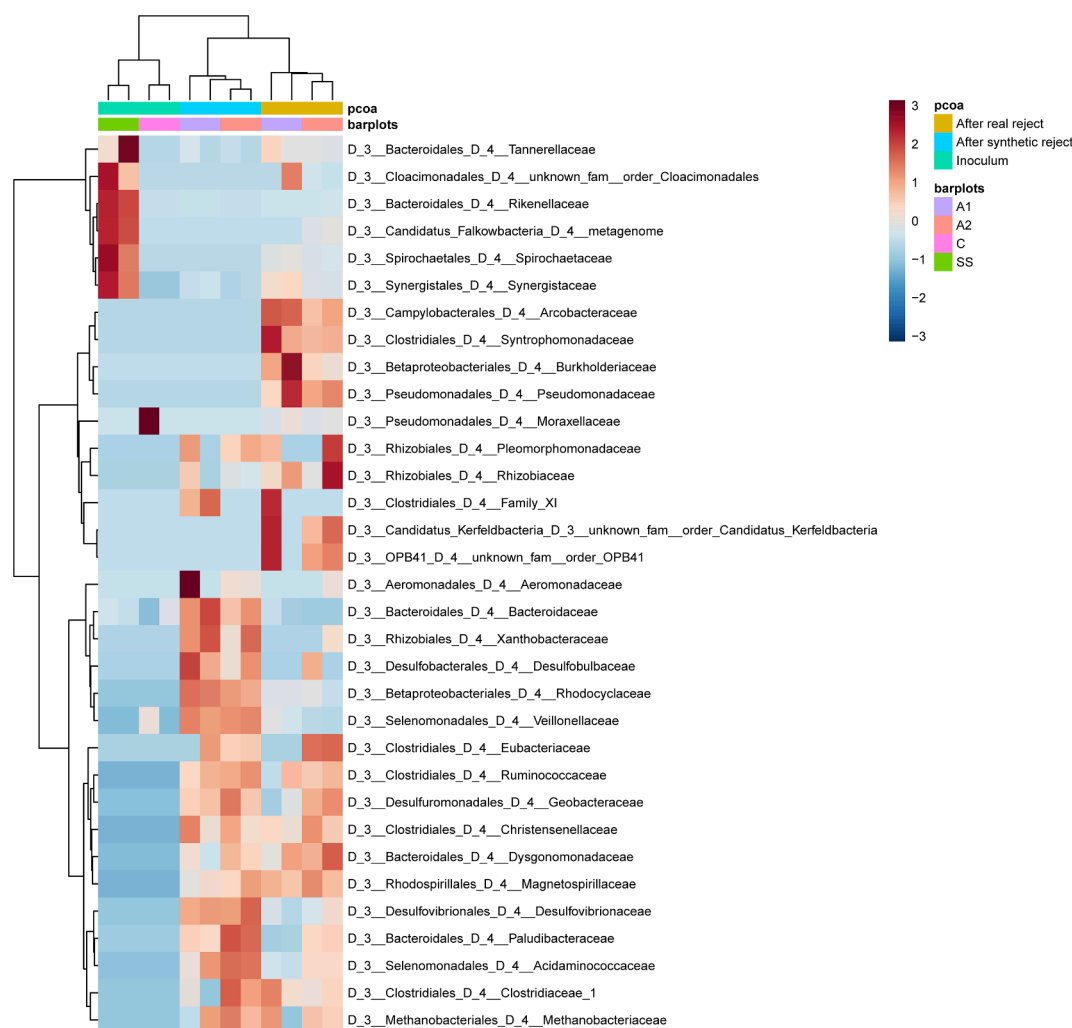


Fig. 4. A heatmap resulting from hierarchical clustering analysis of the microbial communities on bacterial family level from the two inocula (SS = digested sewage sludge; C = compost) on Anode 1 (A1) and Anode 2 (A2) after the continuous mode experiments with synthetic and real reject water. The abundances of different families are scaled to $-3 \dots 3$ individually for each sample. Values for the duplicate samples taken at each sampling point are given separately.

optimisation of the used electrode materials and reduction of inter-electrode distance. The electrical energy consumption in this study was, however, already significantly lower than the combined 25 kWh kg_N⁻¹ required for nitrogen removal in the activated sludge process (12.5 kWh kg_N⁻¹) and fixation for fertiliser use by the traditional Haber-Bosch process (12.5 kWh kg_N⁻¹) [2], indicating the potential of the studied technology for NH₄-N recycling.

3.5. Microbial communities

For the microbial community samples, the analysed amplicon sequence libraries contained on average ca. 92 000 sequences with an average sequence length of 400 bp. Total of 3357 amplicon sequence variants were obtained from these samples. The microbial communities in the inocula and on the electrodes after experiments with synthetic and real reject water were significantly different (PERMANOVA F-value: 5.0422; R²: 0.52841; p < 0.001), as visualised in the heatmap (Fig. 4) and PCoA analysis (Fig. S2). As the anodic microbial community samples were collected directly from the graphite granules used as electrode material, they represent the biomass growing on the electrode surface, thus potentially contributing to the electricity generation.

The digested sewage sludge inoculum was dominated by phylum *Bacteroidetes* (73% relative abundance), with *Firmicutes* (8%) also detected (Table S2). The microbial community of the compost inoculum, on the other hand, was dominated by phylum *Proteobacteria* (50%), followed by *Firmicutes* (38%) and *Bacteroidetes* (12%).

Phylum *Bacteroidetes* was most efficiently enriched at both anodes during the experiments with synthetic reject water, contributing to 56–60% of the microbial communities (Table S2). The other two most detected phyla were *Firmicutes* (27–29%) and *Proteobacteria* (11–14%). After the introduction of real reject water into the system, the relative abundance of phylum *Firmicutes* increased to 32–56%, while the relative abundance of *Bacteroidetes* decreased to 24–48%. The relative abundance of *Proteobacteria* remained relatively unchanged at 14–15%.

When looking at family level, bacteria from phylum *Bacteroidetes* belonged predominantly to families *Paludibacteraceae* (23–39%) and *Bacteroidaceae* (19–30%) at both anodes after the experiments with synthetic reject water (Fig. 4 and Table S2). Members of both families are known to hydrolyse and ferment complex organics [37,38] and have also been previously detected in anodic biofilms in BESs [37,39,40]. For example, a *Bacteroides* sp. from family *Bacteroidaceae* has been found to be able to transfer electrons to Fe(III) during its growth [41], suggesting its capability of extracellular electron transfer. Additionally, family *Veillonellaceae* from phylum *Firmicutes* contributed to 18–22% of the anodic biofilms after experiments with synthetic reject water. Members of family *Veillonellaceae* have also been detected in the anodic communities of microbial fuel cells [42,43].

After the introduction of real reject water into the system, the microbial communities at both anodes changed significantly (Fig. 4 and Fig. S2). The overall shift in the microbial community composition was likely caused by the difference in the chemical composition of the synthetic and real reject water, as well as the introduction of new bacterial species with the real reject water. For example, family *Syntrophomonadaceae* from phylum *Firmicutes*, which was completely absent from both anodes after the experiments with synthetic reject water, was enriched at both anodes to relative abundances of 12–25% with real reject water. At the same time, the decreases in the relative abundance of families *Bacteroidaceae* to 5–11% and *Veillonellaceae* to 7–16% were statistically significant based on the univariate analysis (p < 0.005).

Members of the *Syntrophomonadaceae* family are typically found in anaerobic digesters treating sewage sludge where they are responsible for the β-oxidation of longer-chain monocarboxylic acids to produce acetate and H₂ [44]. Recently, genus *Syntrophomonas* from family *Syntrophomonadaceae* was found to become highly abundant in AD with the addition of conductive materials, and it was reported to be capable of extracellularly transferring electrons originating from the oxidation of

organic matter via direct interspecies electron transfer [45]. This indicates the potential of family *Syntrophomonadaceae* to contribute to electricity generation at the anodes in this study.

The results from the microbial community analysis show that it is possible to enrich specialised and adaptable anodic biofilms for nutrient recovery from reject water from common inocula available everywhere, such as digested sewage sludge and municipal biowaste compost. The change in the microbial community composition when changing from synthetic to real reject water indicates the robustness of the microbial community and its ability to adapt to changing operational conditions. The family level examination revealed several potentially-electroactive bacterial families but additional research into the properties of the bacterial groups identified here is required to confirm their electroactivity.

4. Conclusions

This study demonstrated NH₄-N recovery from digested sewage sludge reject water into a liquid concentrate in a continuously operated 3-chamber bioelectroconcentration cell using reject water as the sole electrolyte. The obtained NH₄-N recoveries were the highest to date reported for a bioelectroconcentration system, peaking at 75.5 ± 2.7% with synthetic and 53.2 ± 4.9% with real reject water. With the optimised operational parameters, NH₄-N was up-concentrated from 1015 ± 48 mg L⁻¹ in synthetic and 665 ± 7 mg L⁻¹ in real reject water to 7483 ± 625 and 6508 ± 438 mg L⁻¹, respectively, in the produced concentrates. Electrical energy requirement for NH₄-N recovery from real reject water varied from 6.1 ± 1.1 to 8.2 ± 3.1 kWh kg_N⁻¹ under the studied operational conditions, which is considerably less than the combined 25 kWh kg_N⁻¹ needed for nitrogen removal in the activated sludge process and fertiliser production using the traditional Haber-Bosch process. 16S rRNA analysis of the anodic biofilms showed the microbial communities were dominated by phylum *Bacteroidetes* in the experiments with synthetic reject water, whereas phylum *Firmicutes* became more abundant when introducing real reject water. Nutrient recovery from reject waters using bioelectroconcentration shows potential for reducing the nitrogen load to WWTPs and thus their energy consumption, but further analysis is required to quantitatively determine the effects on the overall WWTP process.

CRedit authorship contribution statement

Veera Koskue: Conceptualization, Methodology, Investigation, Formal analysis, Visualization, Writing - original draft, Funding acquisition. **Johanna M. Rinta-Kanto:** Formal analysis, Visualization, Writing - review & editing. **Stefano Freguia:** Conceptualization, Methodology, Supervision, Writing - review & editing. **Pablo Ledezma:** Conceptualization, Methodology, Supervision, Writing - review & editing. **Marika Kokko:** Conceptualization, Methodology, Supervision, Writing - review & editing.

Declaration of Competing Interest

The authors declare that they have no known competing financial interests or personal relationships that could have appeared to influence the work reported in this paper.

Acknowledgements

Pablo Ledezma acknowledges an ECR Development Fellowship from The University of Queensland. The authors acknowledge Dr. Maripaz Ventero Martín from The Foundation for the Promotion of Health and Biomedical Research of Valencia Region (FISABIO; Valencia, Spain) for assisting with the DNA extraction and sequencing.

Funding

This work was supported by Maj and Tor Nessling Foundation [grant number 201800132]; and Tampere University Doctoral School supporting Veera Koskue.

Appendix A. Supplementary material

Supplementary data to this article can be found online at <https://doi.org/10.1016/j.seppur.2021.118428>.

References

- [1] M. Sutton, A. Bleeker, C. Howard, M. Bekunda, B. Grizzetti, W. de Vries, H. van Grinsven, Y. Abrol, T. Adhya, G. Billen, E. Davidson, A. Datta, R. Diaz, J. Erisman, X. Liu, O. Oenema, C. Palm, N. Raghuram, S. Reis, R. Scholz, T. Sims, H. Westhoek, Z. FS, Our Nutrient World: The challenge to produce more food and energy with less pollution, *Global Overview Nutrient Manage.*, 2013.
- [2] M. Maurer, P. Schwegler, T.A. Larsen, Nutrients in urine: Energetic aspects of removal and recovery, *Water Sci. Technol.* 48 (2003) 37–46, <https://doi.org/10.2166/wst.2003.0011>.
- [3] G. Billen, J. Garnier, L. Lassaletta, The nitrogen cascade from agricultural soils to the sea (SM), *Philos. Trans. R. Soc. B.* 368 (2013).
- [4] A. Mulder, The quest for sustainable nitrogen removal technologies, *Water Sci. Technol.* 48 (2003) 67–75.
- [5] X. Wu, O. Modin, Ammonium recovery from reject water combined with hydrogen production in a bioelectrochemical reactor, *Bioresour. Technol.* 146 (2013) 530–536, <https://doi.org/10.1016/j.biortech.2013.07.130>.
- [6] C. Fux, H. Siegrist, Nitrogen removal from sludge digester liquids by nitrification/denitrification or partial nitrification/anammox: Environmental and economical considerations, *Water Sci. Technol.* 50 (2004) 19–26, <https://doi.org/10.2166/wst.2004.0599>.
- [7] Y. V. Nancharaiiah, S. Venkata Mohan, P.N.L. Lens, Recent advances in nutrient removal and recovery in biological and bioelectrochemical systems, *Bioresour. Technol.* 215 (2016) 173–185, <https://doi.org/10.1016/j.biortech.2016.03.129>.
- [8] K. Rabaey, J. Rodríguez, L.L. Blackall, J. Keller, P. Gross, D. Batstone, W. Verstraete, K.H. Neelson, Microbial ecology meets electrochemistry: electricity-driven and driving communities, *ISME J.* 1 (2007) 9–18, <https://doi.org/10.1038/ismej.2007.4>.
- [9] B.E. Logan, R. Rossi, A. Ragab, P.E. Saikaly, Electroactive microorganisms in bioelectrochemical systems, *Nat. Rev. Microbiol.* 17 (2019) 307–319, <https://doi.org/10.1038/s41579-019-0173-x>.
- [10] U. Schröder, F. Harnisch, Electrochemical losses, in: K. Rabaey, L. Angenent, U. Schröder, J. Keller (Eds.), *Bioelectrochemical Syst. From Extracell. Electron Transf. to Biotechnol. Appl.*, First edit, IWA Publishing, 2010, pp. 119–133.
- [11] P. Kuntke, K.M. Śmiech, H. Bruning, G. Zeeman, M. Saakes, T.H.J.A. Sleutels, H.V.M. Hamelers, C.J.N. Buisman, Ammonium recovery and energy production from urine by a microbial fuel cell, *Water Res.* 46 (2012) 2627–2636, <https://doi.org/10.1016/j.watres.2012.02.025>.
- [12] P. Ledezma, J. Jermakka, J. Keller, S. Freguia, Recovering nitrogen as a solid without chemical dosing: bio-electroconcentration for recovery of nutrients from urine, *Environ. Sci. Technol. Lett.* 4 (2017) 119–124, <https://doi.org/10.1021/acs.estlett.7b00024>.
- [13] J. Monetti, P. Ledezma, B. Virdis, S. Freguia, Nutrient recovery by bio-electroconcentration is limited by wastewater conductivity, *ACS Omega.* 4 (2019) 2152–2159, <https://doi.org/10.1021/acsomega.8b02737>.
- [14] E. Friedler, D. Butler, Y. Alfiya, Wastewater composition, in: T.A. Larsen, K.M. Udert, J. Lienert (Eds.), *Source Sep. Decentralization Wastewater Manag.*, 1., IWA Publishing, 2013: pp. 241–257.
- [15] P. Ledezma, P. Kuntke, C.J.N. Buisman, J. Keller, S. Freguia, Source-separated urine opens golden opportunities for microbial electrochemical technologies, *Trends Biotechnol.* 33 (2015) 214–220, <https://doi.org/10.1016/j.tibtech.2015.01.007>.
- [16] G. Libralato, A. Volpi Ghirardini, F. Avezù, To centralise or to decentralise: An overview of the most recent trends in wastewater treatment management, *J. Environ. Manage.* 94 (2012) 61–68, <https://doi.org/10.1016/j.jenvman.2011.07.010>.
- [17] M.T. Vu, W.E. Price, T. He, X. Zhang, L.D. Nghiem, Seawater-driven forward osmosis for pre-concentrating nutrients in digested sludge centrate, *J. Environ. Manage.* 247 (2019) 135–139, <https://doi.org/10.1016/j.jenvman.2019.06.082>.
- [18] J. Desloover, A.A. Woldeyohannis, W. Verstraete, N. Boon, K. Rabaey, Electrochemical resource recovery from digestate to prevent ammonia toxicity during anaerobic digestion, *Environ. Sci. Technol.* 46 (2012) 12209–12216, <https://doi.org/10.1021/es3028154>.
- [19] J. Desloover, J. De Vrieze, M. Van De Vijver, J. Mortelmans, R. Rozendal, K. Rabaey, Electrochemical nutrient recovery enables ammonia toxicity control and biogas desulfurization in anaerobic digestion, *Environ. Sci. Technol.* 49 (2015) 948–955, <https://doi.org/10.1021/es504811a>.
- [20] A.J. Ward, K. Arola, E. Thompson Brewster, C.M. Mehta, D.J. Batstone, Nutrient recovery from wastewater through pilot scale electrodiolysis, *Water Res.* 135 (2018) 57–65, <https://doi.org/10.1016/j.watres.2018.02.021>.
- [21] Y. Pan, T. Zhu, Z. He, Minimizing effects of chloride and calcium towards enhanced nutrient recovery from sidestream centrate in a decoupled electrodiolysis driven by solar energy, *J. Clean. Prod.* 263 (2020), 121419, <https://doi.org/10.1016/j.jclepro.2020.121419>.
- [22] S. Barua, B.S. Zakaria, T. Chung, F.I. Hai, T. Haile, A. Al-Mamun, B.R. Dhar, Microbial electrolysis followed by chemical precipitation for effective nutrients recovery from digested sludge centrate in WWTPs, *Chem. Eng. J.* 361 (2019) 256–265, <https://doi.org/10.1016/j.cej.2018.12.067>.
- [23] J. Jermakka, E. Thompson, P. Ledezma, S. Freguia, Electro-concentration for chemical-free nitrogen capture as solid ammonium bicarbonate, *Sep. Purif. Technol.* 203 (2018) 48–55, <https://doi.org/10.1016/j.seppur.2018.04.023>.
- [24] O. Modin, K. Fukushi, K. Rabaey, R.A. Rozendal, K. Yamamoto, Redistribution of wastewater alkalinity with a microbial fuel cell to support nitrification of reject water, *Water Res.* 45 (2011) 2691–2699, <https://doi.org/10.1016/j.watres.2011.02.031>.
- [25] J.M. Haavisto, M.E. Kokko, C.H. Lay, J.A. Puhakka, Effect of hydraulic retention time on continuous electricity production from xylose in up-flow microbial fuel cell, *Int. J. Hydrogen Energy.* 42 (2017) 27494–27501, <https://doi.org/10.1016/j.ijhydene.2017.05.068>.
- [26] F. Meyer, D. Paarmann, M. D'Souza, R. Olson, E.M. Glass, M. Kubal, T. Paczian, A. Rodriguez, R. Stevens, A. Wilke, J. Wilkening, R.A. Edwards, The metagenomics RAST server - a public resource for the automatic phylogenetic and functional analysis of metagenomes, *BMC Bioinform.* 9 (2008) 386, <https://doi.org/10.1186/1471-2105-9-386>.
- [27] V. Koskue, PhD Veera Koskue (mgp90565), MG-RAST. *Metagenomics Anal. Serv.*, 2019. <https://www.mg-rast.org/linkin.cgi?project=mgp90565>.
- [28] M. Rodríguez Arredondo, P. Kuntke, A. ter Heijne, H.V.M. Hamelers, C.J. N. Buisman, Load ratio determines the ammonia recovery and energy input of an electrochemical system, *Water Res.* 111 (2017) 330–337, <https://doi.org/10.1016/j.watres.2016.12.051>.
- [29] M. Rodríguez Arredondo, P. Kuntke, A. ter Heijne, C.J.N. Buisman, The concept of load ratio applied to bioelectrochemical systems for ammonia recovery, *J. Chem. Technol. Biotechnol.* (2019), <https://doi.org/10.1002/jctb.5992>.
- [30] F. Fischer, G. Zufferey, M. Sugnaux, M. Happe, Microbial electrolysis cell accelerates phosphate remobilisation from iron phosphate contained in sewage sludge, *Environ. Sci. Process. Impacts.* 17 (2015) 90–97, <https://doi.org/10.1039/c4em00536h>.
- [31] E. Thompson Brewster, A.J. Ward, C.M. Mehta, J. Radjenovic, D.J. Batstone, Predicting scale formation during electrodiolysis nutrient recovery, *Water Res.* 110 (2017) 202–210, <https://doi.org/10.1016/j.watres.2016.11.063>.
- [32] S.A. Omar, M.A. Abdel-Sater, A.M. Khalil, M.H. Abd-Alla, Growth and enzyme activities of fungi and bacteria in soil salinized with sodium chloride, *Folia Microbiol. Off. J. Inst. Microbiol. Acad. Sci. Czech Repub.* 39 (1994) 23–28, <https://doi.org/10.1007/BF02814524>.
- [33] J.J. Walsh, D.L. Jones, G. Edwards-Jones, A.P. Williams, Replacing inorganic fertilizer with anaerobic digestate may maintain agricultural productivity at less environmental cost, *J. Plant Nutr. Soil Sci.* 175 (2012) 840–845, <https://doi.org/10.1002/jpln.201200214>.
- [34] P. Kuntke, M. Rodríguez Arredondo, L. Widyakristi, A. Ter Heijne, T.H.J. A. Sleutels, H.V.M. Hamelers, C.J.N. Buisman, Hydrogen gas recycling for energy efficient ammonia recovery in electrochemical systems, *Environ. Sci. Technol.* 51 (2017) 3110–3116, <https://doi.org/10.1021/acs.est.6b06097>.
- [35] P. Kuntke, M. Rodrigues, T. Sleutels, M. Saakes, H.V.M. Hamelers, C.J.N. Buisman, Energy-efficient ammonia recovery in an up-scaled hydrogen gas recycling electrochemical system, *ACS Sustain. Chem. Eng.* 6 (2018) 7638–7644, <https://doi.org/10.1021/acssuschemeng.8b00457>.
- [36] M. Rodrigues, T. Sleutels, P. Kuntke, D. Hoekstra, A. ter Heijne, C.J.N. Buisman, H. V.M. Hamelers, Exploiting Donnan Dialysis to enhance ammonia recovery in an electrochemical system, *Chem. Eng. J.* 395 (2020), 125143, <https://doi.org/10.1016/j.cej.2020.125143>.
- [37] B.S. Zakaria, L. Lin, B.R. Dhar, Shift of biofilm and suspended bacterial communities with changes in anode potential in a microbial electrolysis cell treating primary sludge, *Sci. Total Environ.* 689 (2019) 691–699, <https://doi.org/10.1016/j.scitotenv.2019.06.519>.
- [38] A. Ueki, H. Akasaka, D. Suzuki, K. Ueki, Paludibacter propionicigenes gen. nov., sp. nov., a novel strictly anaerobic, Gram-negative, propionate-producing bacterium isolated from plant residue in irrigated rice-field soil in Japan, *Int. J. Syst. Evol. Microbiol.* 56 (2006) 39–44, <https://doi.org/10.1099/ijs.0.63896-0>.
- [39] S. Ishii, Y. Hotta, K. Watanabe, Methanogenesis versus electrogenesis: Morphological and phylogenetic comparisons of microbial communities, *Biosci. Biotechnol. Biochem.* 72 (2008) 286–294, <https://doi.org/10.1271/bbb.70179>.
- [40] J.R. Kim, N.J. Beecroft, J.R. Varcoe, R.M. Dinsdale, A.J. Guwy, R.C.T. Slade, A. Thumser, C. Avignone-Rossa, G.C. Premier, Spatiotemporal development of the bacterial community in a tubular longitudinal microbial fuel cell, *Appl. Microbiol. Biotechnol.* 90 (2011) 1179–1191, <https://doi.org/10.1007/s00253-011-3181-y>.
- [41] A. Wang, L. Liu, D. Sun, N. Ren, D.J. Lee, Isolation of Fe(III)-reducing fermentative bacterium *Bacteroides* sp. W7 in the anode suspension of a microbial electrolysis cell (MEC), *Int. J. Hydrogen Energy.* 35 (2010) 3178–3182, <https://doi.org/10.1016/j.ijhydene.2009.12.154>.
- [42] F. Guo, H. Liu, Impact of heterotrophic denitrification on BOD detection of the nitrate-containing wastewater using microbial fuel cell-based biosensors, *Chem. Eng. J.* 394 (2020), 125042, <https://doi.org/10.1016/j.cej.2020.125042>.
- [43] A.P. Borole, C.Y. Hamilton, T.A. Vishnivetskaya, D. Leak, C. Andras, J. Morrell-Falvey, M. Keller, B. Davison, Integrating engineering design improvements with exoelectrogen enrichment process to increase power output from microbial fuel

- cells, J. Power Sources. 191 (2009) 520–527, <https://doi.org/10.1016/j.jpowsour.2009.02.006>.
- [44] P. De Vos, G.M. Garrity, D. Jones, N.R. Krieg, W. Ludwig, F.A. Rainey, K.-H. Schleifer, W.B. Whitman, eds., *Bergey's Manual of Systematic Bacteriology*. Volume Three: The Firmicutes, Second, Springer, 2009.
- [45] Z. Zhao, Y. Li, Q. Yu, Y. Zhang, Ferroferric oxide triggered possible direct interspecies electron transfer between *Syntrophomonas* and *Methanosaeta* to enhance waste activated sludge anaerobic digestion, *Bioresour. Technol.* 250 (2018) 79–85, <https://doi.org/10.1016/j.biortech.2017.11.003>.